Outskirts of Galaxy Clusters: Intense Life in the Suburbs
Proceedings IAU Colloquium No. 195, 2004
A. Diaferio, ed.

DOI: 10.1017/S1743921304000468

Diffuse intracluster light in 10 clusters at 0.05 < z < 0.31

J. E. Krick and R. A. Bernstein

Department of Astronomy, University of Michigan, Ann Arbor, MI 48109, USA
email: jkrick@umich.edu

Abstract. Surface brightness measurements of the diffuse intracluster light (ICL) in centrally concentrated, relaxed clusters have demonstrated that stars bound only to the cluster potential can contain anywhere from 5 to 50% of the total cluster flux. These stars are a by-product of the evolution of galaxies in clusters, and can be used to constrain models for the structure and evolution of clusters and their member galaxies. The ICL will be an important test of cosmological models as it is a baryonic component of clusters that is likely to evolve with redshift. To learn about these processes we are undertaking a program to measure the characteristics of the ICL (total flux, color, and substructure) as a function of cluster mass, morphology, and redshift. We have obtained data for a sample of 10 clusters at low and moderate redshifts. We discuss here our preliminary results for one cluster in that sample, A3888. With 4-5 hour integration times on-source per filter (V & gunn-r), we reach a 1 sigma surface brightness limit of 29.9 mag/arcsec^2 in the V band. We have identified an intracluster light component that is $\sim$ 10% of total cluster light, extends to 600 kpc from the center of the cluster, and is redder in color than the cluster galaxies ($V - r = 0.4$ near the center, increasing to $V - r = 0.8$ at r = 500 kpc). In addition we find 3 low surface brightness features which are blue ($V - r \simeq 0$), and in total are equivalent to one $m_V = 20.8$ mag galaxy.

1. Introduction

Diffuse intracluster light comes from stars which are bound only to the cluster potential and not to an individual galaxy. Studying the ICL can give insight into the physical processes which drive the formation, morphological evolution, and star formation histories of galaxies. In particular the ICL is interesting because it depends on the structure of the galaxies themselves, the interaction histories of the galaxies, and the details of star formation and how it is triggered inside (or outside) of galaxies. Additionally, the ICL, which is typically not included in the baryon census, will effect the baryon fraction of clusters and the change of baryon fraction as a function of time. If the ICL fraction does indeed evolve with redshift, it will have a systematic effect on the redshift dependence of the baryon fraction. Recent work by Allen, Schmidt, Fabian, & Ebeling (2003) has used a change in baryon fraction with redshift of a few percent to constrain cosmological parameters.

ICL measurements in the literature indicate that the ratio of ICL to total cluster light is $5 - 50\%$ (e.g., Vilchez-Gomez, Pello, & Sanahuja 1994; Bernstein, Nichol, Tyson, Ulmer, & Wittman 1995; Gonzalez, Zabludoff, Zaritsky, & Dalcanton 2000; Feldmeier, Mihos, Morrison, Harding, Kaib, & Dubinski 2004). Theoretical models and N-body simulations over the last 20 years have also predicted similar values for the ICL fraction (e.g., Malumuth & Richstone 1984; Moore, Katz, Lake, Dressler, & Oemler 1996; Dubinski 1998; Mihos 2004). Both the measurements and the modeling have now become sophisticated enough to make real advances in this field.

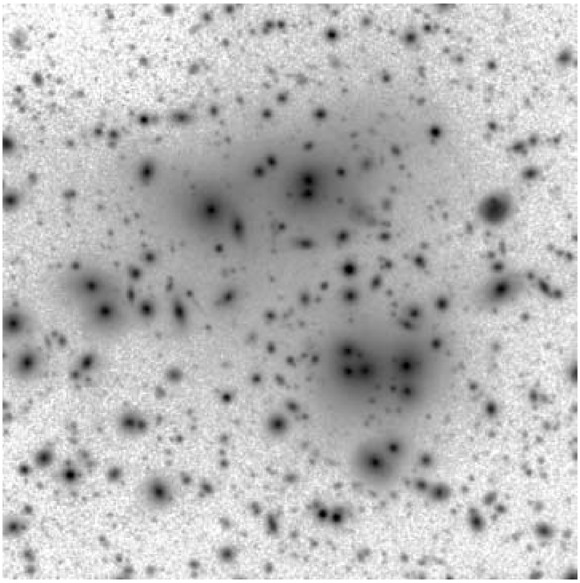

Figure 1. The center of A3888 in V. The grey–scale is linear over the range 20.4–29.5 mag arcsec^{-2}. An extended diffuse component is evident in the cluster core.

2. The program

We have observed a sample of 10 clusters as an addition to the forming statistical sample in the literature. These clusters were selected based on 3 main properties; (1) available X-ray observations giving an estimate of the masses, (2) the clusters are representative of a range in cluster mass, morphology, richness and redshift, and (3) they are at low HI column density and high galactic latitude to avoid the effects of galactic extinction and light (see Table 1). A few selected clusters have lensing mass estimates as a complimentary method of determining cluster mass.

We have fully reduced one cluster in our sample, A3888, for which we have $\sim$ 4.5 hours total integration time on source with the LCO 100" duPont telescope in both V and gunn-r. In addition 1/3 of the total exposure time over the run was devoted to blank sky images to create night sky flats. The data were processed in the standard way with special attention paid to flat fielding and sky subtraction. A large-scale flat fielding accuracy of 0.1% of the sky value is reached to achieve our goal of measuring the ICL to 29.9 mag/arcsec^2 in the V band. Figure 1 shows the fully reduced image of the central Mpc of A3888. It is evident that this cluster does not have a cD galaxy, however the three central clumps of galaxies are confirmed members. These central galaxies are not well fit by deVaucouleurs profiles or any combination of Sersic and exponential disk profiles. This cluster is dynamically active, which will be important in interpreting the flux and substructure in the ICL.

3. Substructure

Using the technique of unsharp masking, we find 3 possible tidal features all within the central 500 kpc of A3888. There are 2 small arcs (10 kpc x 3 kpc) near to the center of the cluster and 1 large (90 kpc x 13 kpc) diffuse, tail-like feature at $\sim$ 500 kpc from the center. These objects are unlikely to be gravitational arcs since they are not oriented tangentially to the cluster distribution. The diffuse nature of the large feature

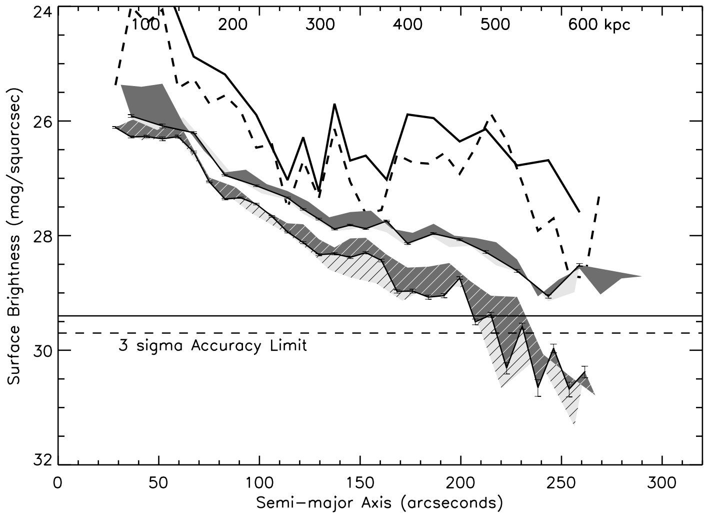

Figure 2. Radial profile of A3888 in V and gunn-r. The solid lines surrounded by shading show our measurement of the SB of the ICL as a function of radius in the r (solid shadings) and V band (hatched shadings). Error bars on the solid lines are standard deviation on the mean in each of the elliptical annuli. As mask size is a concern, we have adjusted the mask size±30% and plotted those surface brightness' as the shaded lines above and below the solid lines respectively. Total cluster flux is shown in the r (solid) and V (dashed) lines. A 3-sigma accuracy limit from the large scale flat fielding is shown for both r (solid) and V(dashed).

also suggests that it is tidal in nature. We cannot yet rule out the possibility that the 2 smaller features are low surface brightness galaxies seen edge-on.

All three features are blue in color, $V - r \simeq 0.0$, implying a young population coming from late-type galaxies. The total flux in these 3 features is equal to one r = 20.8 mag galaxy, which is 10% of an M^* galaxy. Given a cluster crossing time for this cluster of 3.5 Gyr and assuming these tidal features will dissipate in ~ 1 crossing time, over 1 Hubble time approximately $\frac{1}{2}$ of an M^* galaxy will be contributed to the ICL through the visible tidal features.

4. Surface brightness

To measure the flux in the ICL we remove all flux in the image due to detected stars and galaxies. We use SExtractor (Bertin & Arnouts 1996) to identify all sources down to $m_V = 24.8$ mag with sizes greater than 1.5” at a SNR of 5. We determine the PSF of this telescope to a radius of 120” (450 pix) by combining the profiles of super-saturated stars with non-saturated stars. The PSF is well fit by a Moffat function, which is used to subtract all stars from the image. The galaxy profiles, on the other hand, are not easy to quantify as they do not have a simple analytic form. In order to avoid errors from imperfect galaxy subtraction techniques, we mask all galaxies to 2.0 - 2.5 times their isophotal radii as defined by SExtractor. The masks are large enough that mask size has a negligible effect on the inferred ICL as described below.

After subtracting the stars and masking the galaxies, we smooth the image with a 5x5” boxcar, and then fit the resulting image with the IRAF routine ELLIPSE, (see figure 2). ELLIPSE is unable to fit isophotes in the very center where many pixels are masked,

https://doi.org/10.1017/S1743921304000468 Published online by Cambridge University Press

but quickly takes up a position angle similar to that in the x-ray image at larger radii, indicating that the ICL is following the underlying mass distribution of the cluster. Figure 2 also shows 3σ accuracy limits for the large scale flat fielding and background subtraction.

To identify the surface brightness profile of the resolved cluster galaxies we estimate cluster membership based on the color magnitude relation for this cluster. Those galaxies which lie within 1σ of a biweight fit to the color magnitude diagram are taken to be cluster members. In addition to this color cut we have also made a measurement of the contribution due to foreground and background galaxies by measuring the galaxy flux in a background annulus 1Mpc from the center of the cluster. More accurate measurements of cluster membership will come from a luminosity function (LF).

5. Discussion and conclusions

We have identified an intracluster component in A3888 out to 600 kpc from the center of the cluster down to ~ 30.0 mag/arcsec^2 in the V and gunn-r band. We show that this component does not follow the same light profile as the resolved sources, but rather has a steeper surface brightness profile. This ICL component is found to be aligned with the hot gas in the cluster as evidence of its correlation with the underlying mass distribution.

The ICL is redder than the galaxies, implying origins in an older population of stars. We find preliminary evidence for a color gradient in the ICL, where the ICL becomes redder with increasing radius ($V - r = 0.4 - 0.8$).

Comparing the ICL to cluster galaxy flux, we find that the ICL component in A3888 accounts for $\sim 10\%$ of the total cluster flux. A more accurate estimate of cluster flux will come from a LF, for which data has kindly been made available by Pimbblet, Smail, Kodama, Couch, Edge, Zabludoff, & O'Hely (2002). A LF will also provide us with an estimate of the flux from LSB galaxies below our detection threshold, which we are currently unable to disentangle from the ICL.

Reduction of the remaining sample of 9 clusters continues. Once complete, we will be able to examine the exciting physics locked up in the dependence of the ICL on cluster characteristics.

References

Abell, G. O., Corwin, H. G., & Olowin, R. P. 1989, *ApJS*, **70**, 1

Allen, S. W., Schmidt, R. W., Fabian, A. C., & Ebeling, H. 2003 *MNRAS* **342**, 287

Batuski, D. J., Miller, C. J., Slinglend, K. A., Balkowski, C., Maurogordato, S., Cayatte, V., Felenbok, P., & Olowin, R. 1999, *ApJ*, **520**, 491

Bernstein, G. M., Nichol, R. C., Tyson, J. A., Ulmer, M. P., & Wittman, D. 1995 *AJ* **110**, 1507

Bertin, E. & Arnouts, S. 1996 *A&AS*, 117, 393

Busarello, G., Merluzzi, P., La Barbera, F., Massarotti, M., & Capaccioli, M. 2002, *A&A*, **389**, 787

Chen, J., Huchra, J. P., McNamara, B. R., & Mader, J. 1998, *Bulletin of the American Astronomical Society*, **30**, 1307

Ciardullo, R., Ford, H., & Harms, R. 1985, *ApJ*, **293**, 69

Collins, C. A., Guzzo, L., Nichol, R. C., & Lumsden, S. L. 1995, *MNRAS*, **274**, 1071

Couch, W. J. & Newell, E. B. 1984, *ApJS*, **56**, 143

Couch, W. J. & Sharples, R. M. 1987, *MNRAS*, **229**, 423

Couch, W. J., Balogh, M. L., Bower, R. G., Smail, I., Glazebrook, K., & Taylor, M. 2001, *ApJ*, **549**, 820

den Hartog, R. 1995, Ph.D. Thesis

https://doi.org/10.1017/S1743921304000468 Published online by Cambridge University Press

De Propris, R., Couch, W. J., Colless, M., Dalton, G. B., Collins, C., Baugh, C. M., Bland-Hawthorn, J., Bridges, T., Cannon, R., Cole, S., Cross, N., Deeley, K., Driver, S. P., Efstathiou, G., Ellis, R. S., Frenk, C. S., Glazebrook, K., Jackson, C., Lahav, O., Lewis, I., Lumsden, S., Maddox, S., Madgwick, D., Moody, S., Norberg, P., Peacock, J. A., Percival, W., Peterson, B. A., Sutherland, W., & Taylor, K. 2002, *MNRAS*, **329**, 87

Dubinski, J. 1998 *ApJ* **502**, 141

Ebeling, H., Voges, W., Bohringer, H., Edge, A. C., Huchra, J. P., & Briel, U. G. 1996, *MNRAS*, **281**, 799

Feldmeier, J. J., Mihos, J. C., Morrison, H. L., Harding, Kaib, P. N., & Dubinski, J. 2004 *ApJ*, in press

Girardi, M., Borgani, S., Giuricin, G., Mardirossian, F., & Mezzetti, M. 1998, *ApJ*, **506**, 45

Girardi, M. & Mezzetti, M. 2001, *ApJ*, **548**, 79

Gonzalez, A. H., Zabludoff, A. I., Zaritsky, D., & Dalcanton, J. J. 2000 *ApJ* **536**, 561

Kowalski, M. P., Ulmer, M. P., & Cruddace, R. G. 1983, *ApJ*, **268**, 540

Mazure, A., Katgert, P., den Hartog, R., Biviano, A., Dubath, P., Escalera, E., Focardi, P., Gerbal, D., Giuricin, G., Jones, B., Le Fevre, O., Moles, M., Perea, J., & Rhee, G. 1996, *A&A*, **310**, 31

Malumuth, E. M. & Richstone, D. O. 1984 *ApJ* **276**, 413

Mihos, J. C. 2004 In *Clusters of Galaxies: Probes of Cosmological Structure and Galaxy Evolution, from the Carnegie Observatories Centennial Symposia.* (ed. J.S. Mulchaey, A. Dressler, & A. Oemler). Carnegie Observatories Astrophysics Series, p. 278. Cambridge University Press.

Moore, B., Katz, N., Lake, G., Dressler, A., & Oemler, A. 1996 *Nature* **379**, 613

Pimbblet, K. A., Smail, I., Kodama, T., Couch, W. J., Edge, A. C., Zabludoff, A. I., & O'Hely, E. 2002 *MNRAS* **331**, 333

Stein, P. 1996, *A&AS*, **116**, 203

Struble, M. F. & Rood, H. J. 1999, *ApJS*, **125**, 35

Teague, P. F., Carter, D., & Gray, P. M. 1990, *ApJS*, **72**, 715

Vilchez-Gomez, R., Pello, R., & Sanahuja, B. 1994 *A&AS* **283**, 37

Wu, X., Xue, Y., & Fang, L. 1999, *ApJ*, **524**, 22

https://doi.org/10.1017/S1743921304000468 Published online by Cambridge University Press

Table 1: Cluster characteristics

cluster name	ra (J2000) (hr:mm)	dec (J2000) (dd:mm)	l (degrees)	b (degrees)	z	B/M	Richness Class	L_x (0.1–2.4 keV) 10^{44}ergs/s[l]	σ_v km/s	Number of confirmed members	n(HI)[l] $10^{20}\mathrm{cm}^{-2}$	lensing measurement
A4059	23:57	-34:40	356.8	-76.06	0.048[r]	I	1	3.09	845^{+280}_{-140}[t]	45[d,p]	1.1	—
A3880	22:28	-30:34	17.99	-58.50	0.058[r]	II	0	1.86	827^{+120}_{-79}[m]	122[q,f,k]	1.1	—
A2734	00:11	-28:52	19.46	-80.98	0.062[r]	III	1	2.55	628^{+61}_{-57}[m]	127[j,p,k]	1.8	—
A2556	23:13	-21:38	41.37	-66.97	0.087[r]	II-III	1	2.47	1247^{+249}_{-249}[t]	5[e,o,b]	2.0	—
A4010	23:31	-36:30	359.0	-70.60	0.096[r]	I-II	1	5.55	625^{+127}_{-95}[m]	30[j,p]	1.4	—
A3888	22:34	-37:43	3.96	-59.40	0.151[r]	I-II	2	14.52	1102^{+137}_{-107}[n]	69[s]	1.2	—
A3984	23:15	-37:48	359.0	-67.19	0.181[r]	II-III	2	9.18	—	—[f]	1.7	—
A0141	01:06	-24:35	175.3	-85.93	0.23[r]	III	3	12.62	—	—[a]	1.8	Dahle et al. (2002)
AC118	00:14	-30:2	8.90	-81.24	0.308[r]	III	3	22.05	1947^{+292}_{-201}[h]	363[c,g,h]	1.7	Smail et al. (1991)
AC114	22:58	-34:47	8.32	-64.78	0.31[a]	II-III	2	7.0	1388^{+128}_{-71}[n]	380[g,i,h]	2.0	Smail et al. (1991)

Notes: a: Abell, Corwin, & Olowin (1989). b: Batuski et al. (1999). c: Busarello et al. (2002) d: Chen et al (1998). e: Ciardullo, Ford, & Harms, (1985). f: Collins et al. (1995). g: Couch & Newell (1984). h: Couch & Sharpless (1987). i: Couch et al (2001). j: den Hartog (1995). k: De Propris et al. (2002). l: Ebeling et al. (1996). m: Girardi et al. (1998). n: Girardi & Mezzetti (2001). o: Kowalski, Ulmer, & Cruddace, (1983). p: Mazure et al. (1996). q: Stein (1996). r: Struble & Rood (1999). s: Teague, Carter, & Gray, (1990). t: Wu, Xue, & Fang (1999).